

Title	Morphology change from nanocrack into periodic pore array formed by femtosecond laser pulses
Author(s)	Moon, Chiwon; Kanehira, Shingo; Miura, Kiyotaka; Tochigi, Eita; Shibata, Naoya; Ikuhara, Yuichi; Hirao, Kazuyuki
Citation	JOURNAL OF APPLIED PHYSICS (2011), 109(1)
Issue Date	2011-01-01
URL	http://hdl.handle.net/2433/160653
Right	Copyright 2011 American Institute of Physics. This article may be downloaded for personal use only. Any other use requires prior permission of the author and the American Institute of Physics. The following article appeared in JOURNAL OF APPLIED PHYSICS 109, 013517 (2011) and may be found at http://link.aip.org/link/?jap/109/013517
Type	Journal Article
Textversion	publisher

Morphology change from nanocrack into periodic pore array formed by femtosecond laser pulses

Chiwon Moon, Shingo Kanehira, Kiyotaka Miura, Eita Tochigi, Naoya Shibata et al.

Citation: *J. Appl. Phys.* **109**, 013517 (2011); doi: 10.1063/1.3527899

View online: <http://dx.doi.org/10.1063/1.3527899>

View Table of Contents: <http://jap.aip.org/resource/1/JAPIAU/v109/i1>

Published by the [American Institute of Physics](#).

Related Articles

Hardness, yield strength, and plastic flow in thin film metallic-glass

J. Appl. Phys. **112**, 053516 (2012)

Development of nondestructive non-contact acousto-thermal evaluation technique for damage detection in materials

Rev. Sci. Instrum. **83**, 095103 (2012)

Impact fragmentation of aluminum reactive materials

J. Appl. Phys. **112**, 043508 (2012)

Domain fragmentation during cyclic fatigue in 94%(Bi_{1/2}Na_{1/2})TiO₃-6%BaTiO₃

J. Appl. Phys. **112**, 044101 (2012)

Strain rate sensitivity and activation volume of Cu/Ni metallic multilayer thin films measured via micropillar compression

Appl. Phys. Lett. **101**, 051901 (2012)

Additional information on *J. Appl. Phys.*

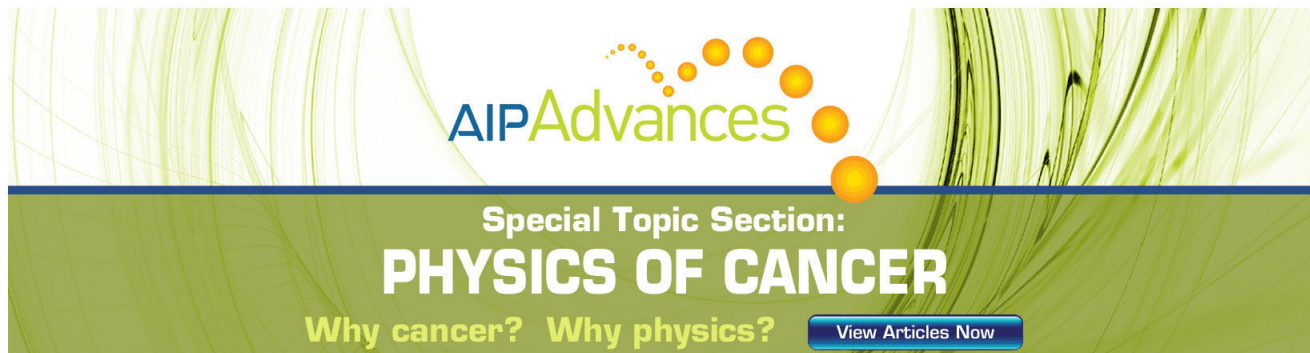
Journal Homepage: <http://jap.aip.org/>

Journal Information: http://jap.aip.org/about/about_the_journal

Top downloads: http://jap.aip.org/features/most_downloaded

Information for Authors: <http://jap.aip.org/authors>

ADVERTISEMENT



AIP Advances

Special Topic Section:
PHYSICS OF CANCER

Why cancer? Why physics? [View Articles Now](#)

Morphology change from nanocrack into periodic pore array formed by femtosecond laser pulses

Chiwon Moon,¹ Shingo Kanehira,^{2,a)} Kiyotaka Miura,¹ Eita Tochigi,³ Naoya Shibata,³ Yuichi Ikuhara,³ and Kazuyuki Hirao¹

¹*Department of Material Chemistry, Graduate School of Engineering, Kyoto University, Nishikyo-ku, Kyoto 615-8510, Japan*

²*Innovative Collaboration Center, Kyoto University, Nishikyo-ku, Kyoto 615-8510, Japan*

³*Institute of Engineering Innovation, School of Engineering, The University of Tokyo, 2-11-16, Yayoi, Bunkyo-ku, Tokyo 113-8656, Japan*

(Received 26 August 2010; accepted 12 November 2010; published online 11 January 2011)

Defects inside single crystals are an important concern because they directly affect the physical or chemical properties of the material, especially in sapphire used as substrates for semiconductors. We have investigated the thermally activated transformations of nanometer-scale cracks and phase transitions inside sapphire by femtosecond laser irradiation and successive heat treatments. The nanocracks transformed into periodic arrays of pores and dislocations that aligned along the $\{1\bar{1}02\}$ planes after heat treatments above 1300 °C. The amorphous phase at the focal point recovered into the initial single crystalline phase after the heat treatments. Our study provides useful information on the recovery behavior of nanometer-scale defects in a single crystal. © 2011 American Institute of Physics. [doi:10.1063/1.3527899]

I. INTRODUCTION

Defects in sapphire single crystal such as dislocations, pores, and cracks, have been extensively studied because they often affect the mechanical and electrical properties of the crystal. Sapphire (α -Al₂O₃) is one of the most important ceramic materials, and recently it has been widely used as substrates for GaN-based semiconductors used for light emitting diodes and laser diodes. However, defects in the sapphire substrate often decrease the luminescence efficiency of the device. Therefore, it is necessary to control the defects in the sapphire substrate to increase the luminescence efficiency. Many studies over the past several decades have been reported on the defects of sapphire, which involve fracture properties, crack propagation and termination, and twinning and slip mechanisms.¹⁻³

In particular, the process of crack reduction through heat treatment is called “crack healing.”⁴ The morphological change in a cylindrical crack in the heat treatment process depends on its aspect ratio, defined as L/D , through the Rayleigh instability,⁵ where L is the length and D is the diameter of the initial crack. The crack splits into a string of spherical pores when $L > \pi D$, or converts directly to a spherical pore when $L < \pi D$ during the heat treatment.⁶

Many effective methods have been used to investigate the crack healing process in sapphire. The most common methods for introducing initial cracks into sapphire include indentation, impact, and abrasion; however, the formation area has been restricted to the surface of the specimens.⁷⁻⁹ Rödel *et al.* produced cracks on the surface of sapphire by ion beam etching and embedded them inside sapphire by thermal bonding to form internal cracks.^{10,11} However, this method involves a complicated procedure for sample prepa-

ration. In addition, the crack widths produced by this method are on the order of a micrometer. There are few reports that demonstrate the morphological changes in cracks formed inside sapphire after heat treatment for cracks at the nanometer scale. That is, selective formation of nanometer-scale cracks inside sapphire and observation of their healing process are very difficult using the conventional mechanical methods.

Recently, the use of femtosecond lasers has attracted considerable attention because they can provide a large amount of energy in a microscopic area inside various transparent materials without surface damage or ablation.¹²⁻¹⁴ The structural changes with a nanometer size often occur after the laser irradiation, which is below the diffraction limit of incident laser beams.¹⁵⁻¹⁷ We previously reported that cracks having a width of approximately 30 nm formed inside sapphire via femtosecond laser irradiation,¹⁸ and their propagation direction and lengths depended on the crystal orientation and laser irradiation conditions, respectively.

Here, we report the thermally activated morphological change in nanometer-scale cracks into periodic defect structures inside sapphire. We introduced nanometer scale cracks inside sapphire using the femtosecond laser, and observed in detail the transformation of the defect structures after heat treatments above 1200 °C using optical and polarizing microscopes and a transmission electron microscope (TEM). We also discuss the formation mechanism of the periodic defect structure in terms of relaxation of residual strain by evaluating the Raman shift around the focal point after the laser irradiation.

II. EXPERIMENTAL

We used (11 $\bar{2}$ 0) sapphire with dimensions of 10 × 10 × 1 mm³ as a sample. A femtosecond laser operating at a wavelength of 780 nm with a pulse frequency of 1 kHz and

^{a)}Electronic mail: kane@collon1.kuic.kyoto-u.ac.jp.

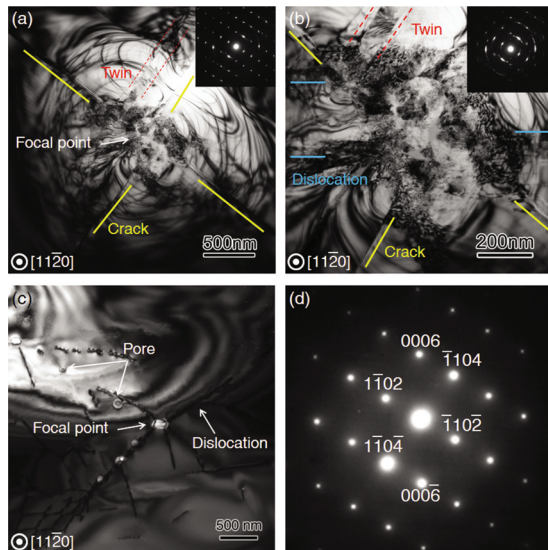


FIG. 1. (Color) Brightfield TEM image of sapphire at the focal point (a) after laser irradiation, (b) its magnified image, and (c) after heat treatment subsequent to the laser irradiation. (d) SAD obtained at the center of the photomodified area after the heat treatment.

a pulse duration of 238 fs, was used as the optical source (IFRIT, Cyber Laser). The pulse energy and number of pulses at the sample location were controlled by a neutral density filter and fast electronic shutter, respectively. A laser beam with a diameter of 5 mm in Gaussian mode was focused at a depth of 50 μm from the sample surface using a microscope objective lens (Nikon, 100 \times) with a numerical aperture (NA) of 0.9. The incident laser beam was normal to the $(1\bar{1}20)$ plane of the sample. The heat treatment was carried out in the range from 1200 to 1500 $^{\circ}\text{C}$ in air to investigate the thermally activated change in the crack morphology. The holding time at each heat treatment temperature was between 1 and 20 h. The structural changes around the focal point after the combination of the laser irradiation and successive heat treatment were observed using an optical, polarizing microscope (Axio Imager, Carl Zeiss) and a TEM (JEOL 2010HC, 200 kV). The TEM sample was prepared by following a standard procedure using ion thinning. We also performed Raman spectroscopy at room temperature with a confocal Raman spectroscope (Nanofinder[®]30, Tokyo Instruments). We evaluated the peak shift and the full widths at half maximum (FWHM) of the spectra obtained from the photomodified area to analyze the residual strain and the crystallinity around the focal point. A frequency-doubled neodymium-doped yttrium aluminium garnet, Nd:Y₃Al₅O₁₂ laser operating at 532 nm was used for the Raman spectroscopy. The spatial and spectral resolutions of the Raman microscope (100 \times objective, NA=0.9) were approximately 275 nm and 0.98 nm, respectively.

III. RESULTS AND DISCUSSION

Figure 1(a) shows a bright-field TEM image of the photomodified area in the sapphire sample after laser irradiation with a pulse energy of 3 μJ . The electron diffraction pattern of the damaged area is also shown in the same figure. A $(1\bar{1}02)$ rhombohedral twin with a width of about 50 nm was

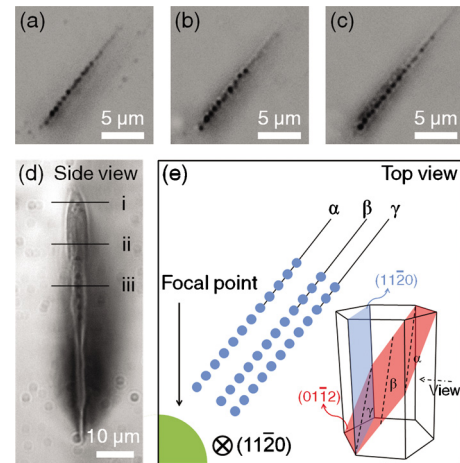


FIG. 2. (Color online) Optical microscope image of the periodic pore structure at different depths of (a) 0, (b) 10, and (c) 20 μm from the focal point after the heat treatment. (d) Side-view optical microscope photo of the photomodified area. (e) Schematic illustration of the aligned pore structures at different depths. The inserted illustration indicates the relationship between $(01\bar{1}2)$ and $(1\bar{1}20)$ planes.

induced near the focus. The rhombohedral twinning deformation, the primary mode of plastic deformation at room temperature,¹⁹ originated from a stress field produced by the laser irradiation. Cracks with a 10 nm width propagated along the $\{1\bar{1}02\}$ planes, which was parallel to the direction of the twin. Therefore, the cracks were probably due to the intersection of multiple twins.² In addition, because fracture surface energy of the $\{1\bar{1}02\}$ planes is the lowest among crystallographic planes in sapphire,²⁰ cracks would preferentially form along these planes. The center of the focal point was extremely deformed after the laser irradiation. Figure 1(b) shows the magnified bright-field TEM image and the selected-area diffraction (SAD) pattern at the center of the focal point. An amorphous phase was found at the center of the damaged area in the TEM image, and the SAD pattern showed halo rings indicating the formation of a polycrystalline structure. Therefore, the extensively deformed area had a diameter of approximately 500 nm and comprised a mixture of an amorphous phase and a polycrystalline structure.^{18,21} In addition, dislocation structures were also observed in the vicinity of the mixed structure.

Figures 1(c) and 1(d) show the bright-field TEM image and the SAD pattern of the photomodified area after the heat treatment at 1500 $^{\circ}\text{C}$ for 10 h, respectively. These images revealed that the amorphous phase recovered into an initial crystalline phase via the heat treatment, due to the stability of the Al₂O₃ crystalline phase at temperatures above 1300 $^{\circ}\text{C}$.²² Additionally, spherical pores were periodically lined up along the crack path, and dislocations were also formed along the crack path. It is suggested that the cracks evolved into arrays of discrete pores and dislocations in order to reduce their surface energy via the heat treatment. The mixture of the pores and dislocations is due to the incomplete recovery of the crack.

Figure 2 shows optical microscope images of the aligned pore structures at different depths of (a) 0, (b) 10, and (c) 20 μm from the focal point after the heat treatment. A side-

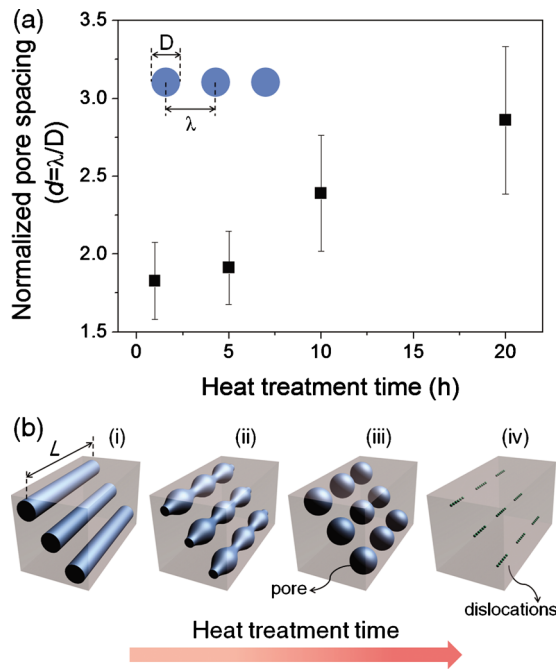


FIG. 3. (Color online) (a) Change in normalized pore spacing ($d = \lambda/D$) as a function of the heat treatment time. (b) Schematic illustration of the change in the crack shape at different heat treatment times.

view optical microscope image after the laser irradiation is also shown in Fig. 2(d). A black dot structure composed of pores or an aggregation of dislocations was observed along the crack path at all depths behind the focal point, although they were independent of each other. This means that the initial crack did not have a planar shape but a discontinuous cylindrical shape, and each crack transformed into discrete pores on a specific plane via heat treatment. Figure 2(e) shows a schematic illustration of the aligned pore structure and the geometric relation between the $(01\bar{1}2)$ and $(11\bar{2}0)$ planes of sapphire. The arrays of the periodic pores at different depths were aligned along the $(01\bar{1}2)$ plane, however, their position varied slightly from α to γ as shown in Fig. 2(e), because the $(01\bar{1}2)$ plane formed an angle of approximately 57.6° with the $(11\bar{2}0)$ plane.

Figure 3(a) shows the relationship between the normalized spacing between pores ($d = \lambda/D$) and the heat treatment time at 1500°C , where λ is the distance between neighboring pores for these arrays and D is the pore diameter. We evaluated the d value from the average of 15 pore arrays at each holding time. The d increased from 1.8 to 2.8 with the increase in the heat treatment time, implying that the crack split into the discrete pores, and each pore shrunk during the heat treatment.

A schematic illustration of the formation process of the periodic pore structure is shown in Fig. 3(b). In general, when the length of the crack, L , was slightly larger than the width D , the crack would evolve into a sphere after the heat treatment via surface diffusion. However, when L was much larger than D , the cylindrical crack in Fig. 3(b), (i), would change into continuous unduloidlike structures as shown in Fig. 3(b), (ii).²³ In the last stage, the initial cracks changed completely into arrays of isolated pores at different depths as

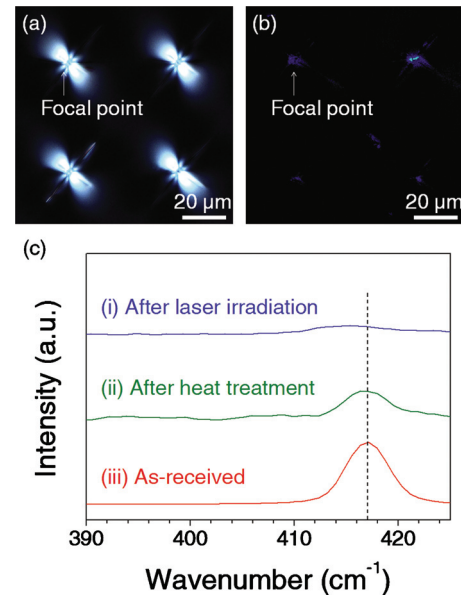


FIG. 4. (Color) (a) Crossed Nicols brightfield image of the photomodified area after laser irradiation, and (b) after the heat treatment subsequent to laser irradiation. (c) Raman spectra obtained from the photomodified area of sapphire (i) after laser irradiation, (ii) after the subsequent heat treatment, and (iii) as-received sapphire. The vertical dashed line at 417 cm^{-1} represents a wave number of A_{1g} vibration in as-received sapphire.

shown in Fig. 3(b), (iii), and the size of each pore decreased, reducing the surface energy after further heat treatment.^{4,24} However, we also observed the periodic dislocation structures as shown in Fig. 3(b), (iv). The formation of these structures is assumed to be as follows: when the cracks propagated inside sapphire by the laser irradiation, the lattices around the cracks were distorted. The lattice misorientation between the two sides of the crack produces misfit strain,²⁵ and finally, dislocations are introduced at the interface of the cracks to relieve the misfit strain when the cracks close.

Figure 4 shows crossed Nicols brightfield images of sapphire (a) after laser irradiation and (b) after successive heat treatment at 1300°C for 5 h. The bright area in Fig. 4(a) indicates the existence of birefringence due to a residual strain around the focal point after the laser irradiation. The asymmetric distribution of the residual strain is ascribed to the difference in fracture surface energies of sapphire. When the femtosecond laser beams were focused inside the sapphire, shock waves were generated and they propagated radially from the focal point. The energy of the shock wave was used to activate the crack formation preferentially on the $\{1\bar{1}02\}$ or $\{1\bar{1}00\}$ planes, which have relatively lower fracture surface energies of all the planes.²⁰ Therefore, the shock wave left a residual strain near a specific crystal plane, resulting in an asymmetric distribution of the birefringence. In the case of Fig. 4(b), the bright area almost disappeared after the heat treatment, which manifested in relaxation of the residual strain around the focal point.

To investigate the relationship between the formation of periodic structures of defects and the relaxation of residual strain at the photomodified area, we examined Raman spectra at the focal point. Figure 4(c) shows Raman spectra at the

TABLE I. Wave numbers at the center peak and the corresponding FWHM of Raman spectra in Fig. 4(c).

	Peak position (cm^{-1})	FWHM (cm^{-1})
As-received	417	3.60
After laser irradiation	415	11.2
After annealing	416	5.50

photomodified area of sapphire after the laser irradiation Fig. 4(c), (i), and successive heat treatment Fig. 4(c), (ii). The spectrum of as-received sapphire is also shown Fig. 4(c), (iii), as a reference. Raman peaks of the sapphire were detected at 378, 417, and 645 cm^{-1} in all the cases. We chose the wave number of 417 cm^{-1} as a criterion originating from Raman-allowed A_{1g} vibration of sapphire because it showed the strongest intensity among the Raman active phonon modes in the $(11\bar{2}0)$ plane of sapphire.²⁶ Table I lists the wave numbers at the center peak and the corresponding FWHM of Raman spectra in Fig. 4(c), and the error is approximately 0.98 nm. The FWHM were calculated with respect to a baseline obtained by drawing a tangent line to the spectrum between 300 and 800 cm^{-1} . The wave number at the center peak showed a redshift from 417 to 415 cm^{-1} after the laser irradiation due to tensile stress; however, it showed a blueshift from 415 to 416 cm^{-1} after the heat treatment. It was confirmed that the residual strain at the photomodified area was predominantly relaxed by the heat treatment, which was in accordance with the results of our polarizing microscope observation. In addition, the FWHM increased from 3.60 to 11.2 cm^{-1} after laser irradiation, indicating the decrease in crystallinity at the photomodified area presumably due to the amorphization or the crack formation by the laser irradiation.²⁷ On the other hand, the FWHM decreased from 11.2 to 5.50 cm^{-1} after the heat treatment, indicating that the crystallinity of the area almost recovered due to the recrystallization.²⁸ The incomplete re-

covery of the crystallinity after the heat treatment was attributable to the residual dislocation structures around the focal point, as shown in Fig. 1(b).

Figure 5(a) shows optical microscope images after heat treatment at 1500 °C with different holding times. A dark circle (i) was observed at the center of the photomodified area after 1 h due to the existence of the amorphous phase and dislocations. In addition, the initial cracks partly closed and changed into the pore arrays (ii). However, the dark circle became less distinct as the heat treatment time increased and finally disappeared after 20 h due to the recrystallization. Additionally, most of the crack healed and the array of discrete pores could be clearly observed after 20 h. Figure 5(b) shows the result of periodic pore formation under different heat treatment conditions. We noticed that the formation of the pore array strongly depended on the holding temperature; the formation of the periodic structures required heat treatment above 1300 °C. Generally, the mobility of atoms in sapphire is enhanced at 1300 °C, which corresponds to a brittle-to-ductile transition temperature.^{8,29} The atomic diffusion process is accelerated at temperatures over 1300 °C because the formation of the periodic pore structures depend on the atomic diffusion accompanied with the decrease in the surface energy. Therefore, we estimated that the critical temperature for the formation of the periodic structure was 1300 °C.

IV. CONCLUSION

In summary, we presented the morphological changes in the internal cracks in sapphire and the formation of dislocation structures under a heat treatment process after femtosecond laser irradiation. The amorphous phase and cracks that had formed inside sapphire via laser irradiation transformed respectively into a crystalline phase and an array of discrete pores after successive heat treatments above 1300 °C. In addition, periodic dislocation structures were also formed along a specific crystal orientation. The transformation from the cracks to the pore arrays was driven by the atomic diffusion during the heat treatment, which decreased the surface energy of the cracks. A Raman survey revealed that most of the lattice strain at the focus was relieved via the heat treatment, although residual strain was produced around the dislocation structures. The analysis of directionally aligned dislocation structures is necessary to clarify the characteristics of defects in sapphire.

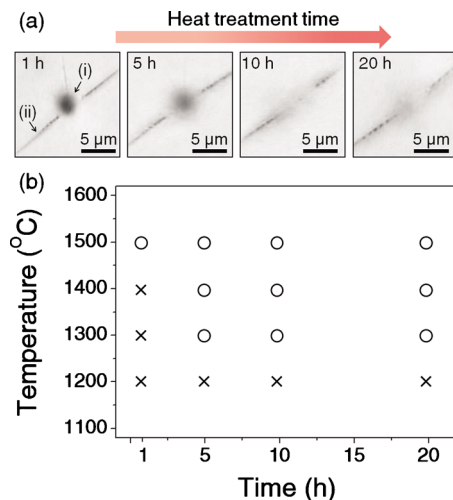


FIG. 5. (Color online) (a) Optical microscope images at the focal point after the heat treatment at 1500 °C for 1, 5, 10, and 20 h. (b) Results of periodic pore structure under various heat treatment temperatures and times.

- ¹J. Castaing, A. He, K. P. D. Lagerlof, and A. H. Heuer, *Philos. Mag.* **84**, 1113 (2004).
- ²A. H. Heuer, *Philos. Mag.* **13**, 379 (1966).
- ³K. P. D. Lagerlof, J. Castaing, P. Pirouz, and A. H. Heuer, *Philos. Mag. A* **82**, 2841 (2002).
- ⁴T. K. Gupta, *J. Am. Ceram. Soc.* **61**, 191 (1978).
- ⁵L. Rayleigh, *Proc. R. Soc. London, Ser. A* **90**, 324 (1914).
- ⁶F. Nichols, *J. Mater. Sci.* **11**, 1077 (1976).
- ⁷J. H. Choi, D. Y. Kim, B. J. Hockey, S. M. Wiederhorn, C. A. Handwerker, J. E. Blendell, W. C. Carter, and A. R. Roosen, *J. Am. Ceram. Soc.* **80**, 62 (1997).
- ⁸H. S. Kim and S. Roberts, *J. Am. Ceram. Soc.* **77**, 3099 (1994).
- ⁹R. Nowak and M. Sakai, *Acta Metall. Mater.* **42**, 2879 (1994).
- ¹⁰J. D. Powers and A. M. Glaeser, *J. Am. Ceram. Soc.* **83**, 2297 (2000).
- ¹¹J. Rödel and A. M. Glaeser, *J. Am. Ceram. Soc.* **73**, 592 (1990).
- ¹²G. J. Lee, J. Park, E. K. Kim, Y. Lee, K. M. Kim, H. Cheong, C. S. Yoon,

- Y. D. Son, and J. Jang, *Opt. Express* **13**, 6445 (2005).
- ¹³K. Miura, J. R. Qiu, S. Fujiwara, S. Sakaguchi, and K. Hirao, *Appl. Phys. Lett.* **80**, 2263 (2002).
- ¹⁴K. Miura, J. R. Qiu, H. Inouye, T. Mitsuyu, and K. Hirao, *Appl. Phys. Lett.* **71**, 3329 (1997).
- ¹⁵S. Kanehira, K. Miura, K. Fujita, K. Hirao, J. Si, N. Shibata, and Y. Ikuhara, *Appl. Phys. Lett.* **90**, 163110 (2007).
- ¹⁶M. Shen, J. E. Carey, C. H. Crouch, M. Kandyla, H. A. Stone, and E. Mazur, *Nano Lett.* **8**, 2087 (2008).
- ¹⁷Y. Shimotsuma, P. G. Kazansky, J. R. Qiu, and K. Hirao, *Phys. Rev. Lett.* **91**, 247405 (2003).
- ¹⁸C. Moon, S. Kanehira, M. Nishi, K. Miura, T. Nakaya, E. Tochigi, N. Shibata, Y. Ikuhara, and K. Hirao, *J. Am. Ceram. Soc.* **92**, 3118 (2009).
- ¹⁹T. Wermelinger, C. Borgia, C. Solenthaler, and R. Spolenak, *Acta Mater.* **55**, 4657 (2007).
- ²⁰S. M. Wiederhorn, *J. Am. Ceram. Soc.* **52**, 485 (1969).
- ²¹S. Juodkazis, K. Nishimura, H. Misawa, T. Ebisui, R. Waki, S. Matsuo, and T. Okada, *Adv. Mater.* **18**, 1361 (2006).
- ²²C. W. White, L. A. Boatner, P. S. Sklad, C. J. McHargue, J. Rankin, G. C. Farlow, and M. J. Aziz, *Nucl. Instrum. Methods Phys. Res. B* **32**, 11 (1988).
- ²³F. A. Nichols and W. W. Mullins, *J. Appl. Phys.* **36**, 1826 (1965).
- ²⁴A. M. Glaeser, *Mater. Lett.* **5**, 239 (1987).
- ²⁵Y. Li, G. C. Weatherly, and M. Niewczas, *J. Appl. Phys.* **98**, 013522 (2005).
- ²⁶S. P. S. Porto and R. S. Krishnan, *J. Chem. Phys.* **47**, 1009 (1967).
- ²⁷J. W. Ager, D. K. Veirs, and G. M. Rosenblatt, *Phys. Rev. B* **43**, 6491 (1991).
- ²⁸H. Richter, Z. P. Wang, and L. Ley, *Solid State Commun.* **39**, 625 (1981).
- ²⁹M. L. Kronberg, *J. Am. Ceram. Soc.* **45**, 274 (1962).